



AFM SILICA-PROBING OF CHARGE DISTRIBUTION ON QUARTZ (0001) AND SAPPHIRE (0001) SURFACES

Gulnihal Yelken^{1,*}, Mehmet Polat

¹Izmir Institute of Technology, Department of Chemical Engineering, Urla Izmir, Turkey

(This article was presented first to the PPM2017, then submitted to JOTCSB as a non-peer-reviewed article)

Abstract: A quantitative prediction of the interactions between surfaces in electrolyte solutions is extremely important in numerous physico-chemical systems. Experimental *in-situ* measurements of these interactions are now possible with AFM down to sub-nanonewton levels. The current methods, whether electrophoretic or titration origin, provides only an average charge or potential value for the system under consideration. In this study, AFM was employed to estimate the surface charge or potential distribution of selected metal oxides using a silica colloid probe. The surface maps obtained show very good agreement with the average charge/potentials values from the literature and recent work.

Cite this: Yelken G, Polat M. AFM SILICA-PROBING OF CHARGE DISTRIBUTION ON QUARTZ (0001) AND SAPPHIRE (0001) SURFACES. Journal of the Turkish Chemical Society, Section B: Chemical Engineering. 2017;1(sp. is. 2):25-34.

*Corresponding author: gulnihal.yelken@gmail.com

INTRODUCTION

Colloidal systems are widely encountered in minerals, ceramics, environment, biology, cosmetics, and pharmaceutical applications where homogeneity, stability, rheology, plasticity or forming characteristics of the system may be extremely important. Control and manipulation of these properties are directly related to the interactions among the particles which constitute these systems.

The two main components of interparticle interaction are van der Waals and Electrical Double Layer (EDL) forces. Interplay of these two components have been formalized by the DLVO Theory [Derjaguin, B.V. and Landau, L., 1941; Verwey, E.J.W. and Overbeek, J.T.G. 1948]. Electrophoretic potential measurements and colloidal titration methods are widely employed to determine quantitatively this charge in a colloidal system. However, these methods yield only an average charge for the surface which leads to assumption that the charge on the surface is homogeneously distributed. It is obvious that use of such an assumption can only approximate the actual mechanism and magnitude of the interactions between surfaces and dissolved species. This shortcoming is simply born from a lack of a better method for determining the actual charge distribution on the surface. [Hoek, E. M. V and Agarwal, G. K, 2006, Meagher, L *et al.*, 1999; Franks, G.V., Meagher, L., 2003; Nowostawska, U., 2005].

Quantitative force measurement using AFM between two surfaces (a cantilever tip or a colloid particle and the surface of interest) have been widely used in numerous studies [Binnig *et al.*, 1986, Ducker, W.A *et al.*, 1991, Butt, H., 1991, 2010; Larson, I. *et al.*, 1993, 1997]. In this paper, we will demonstrate that an Atomic Force Microscope (AFM) can be employed as a physico-chemical probe to yield information on the distribution of electrostatic charges on well-defined oxide surfaces. The net force measured by the AFM at a given point on the surface under carefully maintained solution conditions was separated into its component forces. This information was then employed to estimate the surface potential with proper application of relevant theories and methods. Repeating the measurement on multiple points on the surface generated a 3-D distribution of surface potentials.

MATERIALS

Smooth planar oxide surfaces, quartz 0001 and sapphire 0001 single crystals (MTI, CA, USA) were used as substrates. The coding of the silica sample measured physical properties of the powders is Admatech, Japan, Admafine SO-E6. Rectangular silicon cantilevers (TL-FM-20, Nanosensors (California, USA) were used in the force measurement and employed as charge probes (Figure 1).

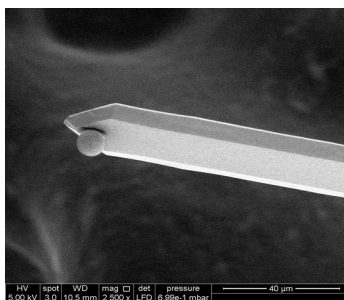


Figure 1: A view of one of the colloidal probe attached rectangular silicon cantilevers (TL-FM-20, Nanosensors (California, USA) used in the force measurements.

Zeta potential measurements were obtained in 10^{-3} M KCl solutions, and the results are presented in Figure 2 for powder which have been used as colloidal probe [Yelken,G. and Polat,M. 2014]. Hamaker Constant analysis are very important in the AFM measurements. The Hamaker Constants of the interacting bodies are for the oxides, $A_{\text{silica}}=1.02 \cdot 10^{-20}$ J; $A_{\text{sapphire}}= 3.67 \cdot 10^{-20}$ J) used in this study [Bergström,L., 1997].

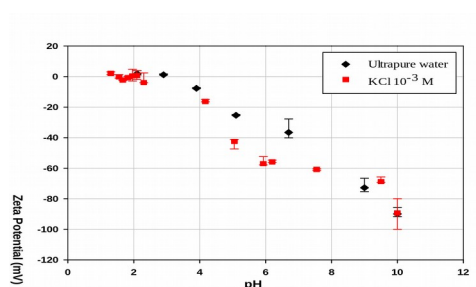


Figure 2: Results of the zeta potential measurements for silica powder. (*Those symbols which seem to have no error bars have errors smaller than the symbol size*).

METHODS

A Nanomagnetics AFM equipped with a custom-made liquid cell was employed in the force measurements in aqueous media. Due to the very sensitive nature of the work, several procedures had to be developed prior to carrying out accurate, reliable and reproducible force measurements. A brief explanation of these procedures is as follows:

The substrates, the silicon nitride probes, and the liquid cell were all subjected to an extensive cleaning procedure before each test. The procedure involved pre-washing in water and ethanol, treatment with ultrasound, radiation with UV to remove residual surface contaminant, re-washing with ethanol and rinsing with water and finally conditioning for 10 minutes in the experimental solution. Though the manufacturer provides an average spring constant for a batch of cantilevers, the exact spring constant value was required for each cantilever for accurately converting the cantilever signal from the AFM to actual force data. Therefore, individual spring constant of each cantilever (k) was determined using Sader's method [Sader, J.E., 1999].

It can be seen that though the average spring constant for the population of the cantilevers value 2.06 which provided by the company nominal value is 2.8 N/m, there was a scatter (between 1.72 and 2.46) in the spring constants of individual cantilevers, corresponding to an error of about 5.5%.

Estimation of Surface Potential from a Comparison of F_t and F_{AFM} : An illustrative actual force-distance curve obtained from the AFM for the silica substrate and silicon nitride tip (F_{AFM}) is given in Figure 3 as symbols. The first-guesses of the theoretical force-distance curves (F_t) for the data are also presented in the figure as solid lines for constant potential and constant charge conditions. The parameters which are kept constant for generating the theoretical curves are given below the figure. It should be noted that the only parameter varied for approaching the theoretical curves to the actual force curve was the surface potential of silica, ψ_{SiO_2} . The procedure outlined above was repeated until a best fit line was obtained for the force-distance data which yielded the best-estimate surface potential for the surface for that measurement. All calculation was made by Polat, M. and Polat H., 2010. Then, the procedure was repeated on multiple points on the surface as follows: Initially five boxes with dimensions of $1 \times 1 \mu\text{m}$ were selected on a $5 \times 5 \mu\text{m}$ area on the surface, four in corners and one in the middle. On each box, force measurements were carried out on 16 points are $10 \mu\text{m}$ away from each other on x and y directions. Each of these 16 measurements at a given point was repeated 3 times to ensure reproducibility. This data was then used to obtain the potential contours of the surface.

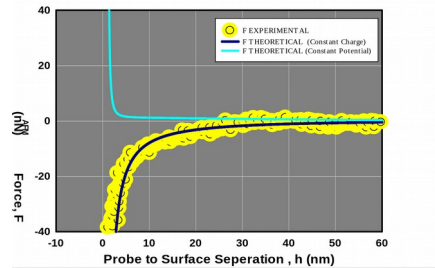


Figure 3: Force-distance data (F_{AFM}) obtained at with silicon nitride tip on silica at pH 10 and 10^{-3} M KCl. The solid lines gives a first-guess curves for theoretical force-distance curves for constant potential and constant charge conditions.

The parameters kept constant obtaining the theoretical force-distance curves:: $k=2.06$ N/m, $A_{132}=1.0210^{-20}$ J; $C_0= 10^{-3}$ M KCl ; $z=1:1$; $T= 293.15$ K). The parameter varied in adjusting the theoretical lines : ψ_{SiO_2}

RESULTS AND DISCUSSION

AFM force measurements were carried out in the liquid cell of the AFM using the cleaning and data acquisition and processing procedures outlined above. The electrolyte solution strength was kept constant in all experiments at 10^{-3} M with KCl.

Measurements were carried out for two well-defined substrates (silica and alumina single crystals) at three different pH values of 2, 6, 10. The results are presented in Figure 4 for quartz and Figure 5 for sapphire substrates. The parameters related to these figures are presented in Table 1. Table also shows the numerical values of the surface potentials and the potential ranges observed on the quartz and sapphire surfaces.

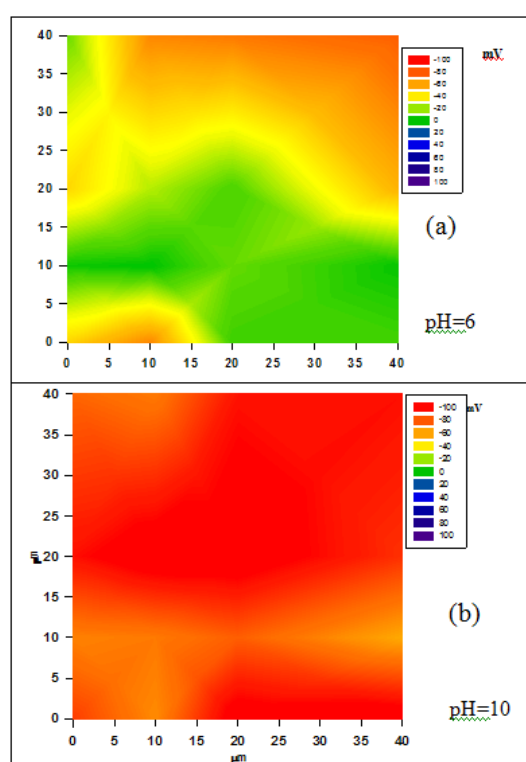


Figure 4: The Surface potential distributions on a 5x5 μm portion of the quartz (0001) surface Silica colloidal probe at various pH values in 10^{-3} M KCl solution. (Spring constant $k= 2.06$ N/m; 10^{-3} M KCl solution; $T=20^{\circ}\text{C}$; $A=1.02 \cdot 10^{-20}$)

It can be seen from Figure 4 and Table 1 that the quartz surface has an average surface potential of 0 mV at pH 2. However, this potential is not evenly distributed on the surface. The potentials on quartz substrate vary between -10 mV and +10 mV. At pH 6, the quartz surface seems to be becoming more negative with surface potentials changing between 0 and -40 mV. The average surface potential for pH 6 is -30 mV. When pH is increased to 10, the quartz surface becomes dominantly negative. In this case, the surface potentials vary between -80 and -100 mV while the average surface potential drops to -90 mV.

Table 4: Experimental Parameters, average potentials and potential ranges for the silica and sapphire surfaces.

	Silica	Alumina
Experimental Parameters		
C_0 (KCl)		10^{-3} M
Z		1:1
T		293.15 K
R Probe ¹		6 nm
A_{132}^2	$1.06 \cdot 10^{-20}$ J	$3.67 \cdot 10^{-20}$ J
$\zeta_{Si_3N_4}^3$ @pH=6		+50 mV
$\zeta_{Si_3N_4}^3$ @pH=10		-60 mV
AFM Measured Average Surface Potentials,		
	mV*	
y_{avg}^4 @pH=6	-30	-30
y_{avg}^4 @pH=10	-90	-60
Measured Surface Potential Ranges, mV*		
y^4 @pH=6	-40 / 0	-10 / -40
y^4 @pH=10	-100 / -80	-65 / -50

1. Measured radius of the Si_3N_4 probe using SEM
2. from Bergstrom [30]
3. Measured using zeta sizer Model Malvern Nano-Zs
4. Average potentials obtained from the potentials measured by AFM on 45 separate locations on the silica and sapphire substrates (see also Figures 4 and 5)
5. Potential ranges for the averages given in 4 above (see also Figures 4 and 5)

For the sapphire substrate, the surface is predominantly positive at a pH of 2 with an average surface potential of +40 mV with a range between +30 and +45 mV as seen in Figure 5. The sapphire surface loses this positive potential significantly when the pH is increased to 6. The average surface potential is -30 mV in this case with a spread of the potentials between -10 and -40 mV. The surface becomes negatively charged at pH 10 such that the the average surface potential drops to -60mV. The sapphire surface at this pH shows a distribution of potentials between -50 and -65 mV.

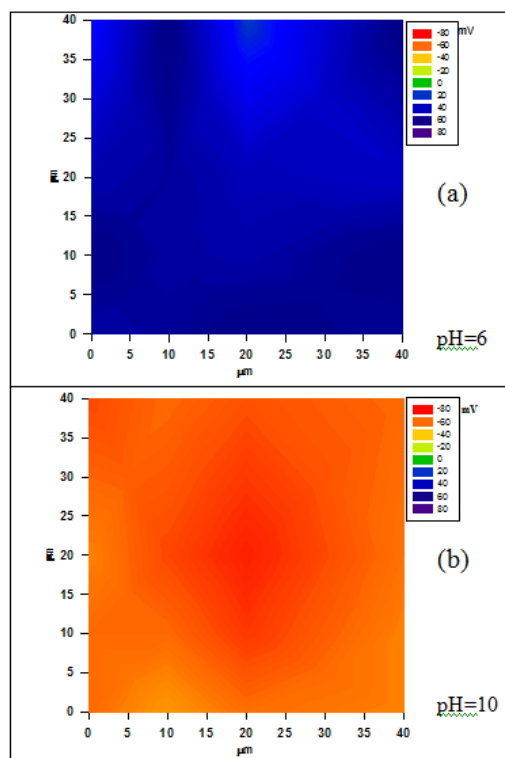


Figure 5: Surface potential distributions on a 5x5 μm portion of the sapphire (0001) surface at various pH values in 10^{-3} M KCl solution. (Spring constant $k=2.06$ N/m; 10^{-3} M KCl solution; $T=20^{\circ}\text{C}$; $A=3.67 \cdot 10^{-20}$ J)

In Figure 6, the average surface potentials with error bars on the quartz surface obtained from the contour graphs (Figure 4) are plotted against the electrophoretic data obtained for the silica and quartz powders. It can be seen that the average surface potentials obtained for the quartz surface (filled circles) at different solution pH agree quite well with the zeta potential data, especially at the acidic range. There seems to be a disagreement between the zeta potentials and the average surface potential of the quartz surface at pH 10. This disagreement can be explained by the possible hydration of the surface at this high pH [Polat et. al, 2006] observed previously that a hydrated surface layer which may develop at high pH values can act as a physical barrier during the approach of the surfaces. Under these conditions authors stated that use of the DLVO theory may not be applicable.

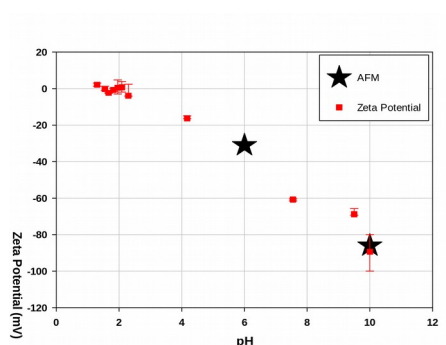


Figure 6: A comparison of the zeta potential measurements for the quartz/silica powders (open symbols-reproduced from Figure 2) with the surface-averaged AFM potential measurement obtained on a quartz single crystal surface (filled symbols-obtained from Figure 4).

In Figure 7, the average surface potentials for the sapphire surface obtained from the contour graphs of Figures 5 are plotted against the zeta potentials for various alumina powders. It can be seen that the average surface potentials obtained for the sapphire surface (filled circles) at different solution pH seem to be lower than the measured zeta potentials at all pH values such that the point of zero charge is around 5.2 for the sapphire surface as opposed to the point of zero charge of around 8.5 for the powders.

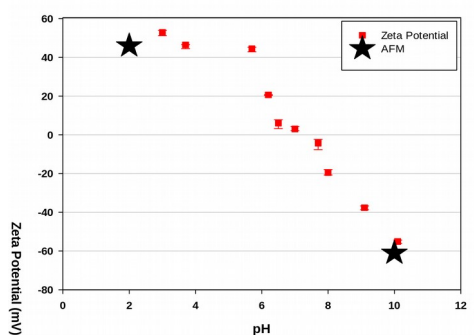


Figure 7: A comparison of the zeta potential measurements for the alumina powders (open symbols-reproduced from Figure 2) with the surface-averaged AFM potential measurement obtained on a single crystal surface (filled symbols-obtained from Figure 5).

Using a streaming potential technique, [Franks and Meagher 2003] observed that single crystal sapphire (0001) surface showed a point of zero charge of 5.2. The streaming potential data obtained by these authors are plotted against the AFM-measured surface potentials presented in Figure 8 for the sapphire surface. It can be seen that the streaming potential values of the sapphire surface agrees quite well with the surface averages of the potential values determined by the methods developed in this paper using the AFM as a charge probe.

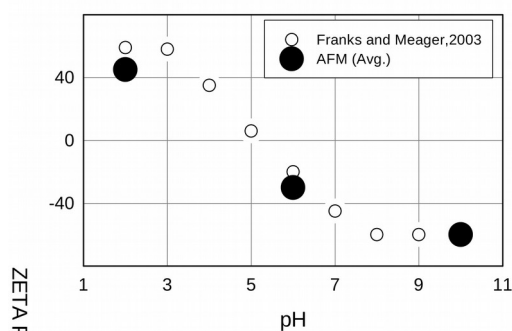


Figure 8: Surface potential of 0001 sapphire single crystal as a function of pH from streaming potential from Franks and Meager [26] (open circles) and from the AFM measurements in this work (filled circles-reproduced from Figure 7).

CONCLUSIONS

In this work, we employed atomic force microscopy to determine the surface potentials on various locations on selected metal oxide surfaces in aqueous solutions in order to estimate the potential distribution of the surface in form of a potential map.

The method is based on measuring the interaction forces between the AFM tip and a desired surface at multiple points and correlating the measured force with the DLVO theory to predict the surface potential at each point. This use of the AFM is novel but requires very careful experimental design and careful use of available theories.

The results presented in this work demonstrate that within the bounds of the applied theory the surface potential distributions predicted with the AFM agree quite well with the data from other independent electrophoretic measurements.

ACKNOWLEDGEMENTS

The support from The Scientific and Technological Research Council of Turkey (TUBITAK) under the Project Grant TUBITAK 109T695 is acknowledged.

REFERENCES

- Bergström, L., Ad. Colloid and Interface Science. 70 (1997) 125.
- Binnig, G., Quate, C. F., Gerber, Ch., Phys. Rev. Lett. 56 (1986) 930.
- Butt, H., Biophys. J. 60 (1991) 1438.
- Butt, H., Kappl, M., Surface and Interfacial Forces, WILEY-VCH Verlag GmbH, Weinheim, 2010.
- Derjaguin, B.V., Landau, L., Physicochim. URSS 14 (1941) 633.
- Ducker, W.A. Senden, T.J. Pashley, R.M. Nature. 353 (1991) 239.
- Franks, G.V., Meagher, L., Colloids and Surfaces A. Physicochem. Eng. Aspects. 214 (2003) 99
- Hoek, E. M. V Agarwal, G. K., J. Colloid Interface Sci. 298 (2006) 50.

Larson, I Drummond, C.J. Chan, D.Y.C Grieser, J. Am. Chem. Soc. 115 (1993) 11885.

Larson, I Drummond, C.J. Chan, D.Y.C Grieser, F., J. Am. Chem. Soc. 99 (1995) 2114.

Larson, I Drummond, C.J. Chan, D.Y.C Grieser, F., Langmuir. 13 (1997) 2109.

Meagher, L., Franks, G.V., Gee, M.L., J. Scales, Colloids and Surfaces A. Physicpchem. Eng. Aspects. 146 (1999) 123.

Nowostawska, U., Sander, S.G., Hunter, K.A., Colloids and Surfaces A. Physicpchem. Eng. Aspects. 266 (2005) 200.

Polat, M., Sato, K., Nagaoka, T., Watari, K., J. Colloid Interface Sci. 304 (2006) 378.

Polat, M., Polat, H., J. Colloid Interface Sci. 341 (2010) 178.

Sader, J.E, Chon, J.W.M, Mulvaney, P., Rev. Sci. Instrum. 70 (1999) 3967.

Verwey, E.J.W. , Overbeek, J.T.G., Theory and Stability of Lyophobic Colloids, Elsevier, Amsterdam, 1948.

Yelken, G.O., Polat, M., Applied Surf. Sci., 301, 2014, 149-155.